Elastic versus alloying effects in Mg-based hydride films

Andrea Baldi*
DIFFER - Dutch Institute for Fundamental Energy Research, De Zaale 20, 5612 AJ Eindhoven, The Netherlands

Lennard Mooij, Valerio Palmisano, Herman Schreuders, and Bernard Dam
Delft University of Technology, Van der Maasweg 9, 2629 HZ Delft, The Netherlands

Gopi Krishnan
Amrita Center for Nanosciences and Molecular Medicine, Amrita Vishwa Vidyapeetham, Kochi, Kerala 682041, India

Bart J. Kooi
University of Groningen, Nijenborgh 4, 9747 AG Groningen, The Netherlands

Ronald Griessen
VU University, De Boelelaan 1081, 1081 HV Amsterdam, The Netherlands
(Dated: October 26, 2018)

Magnesium thin films covered with a layer of Pd absorb hydrogen at much higher pressures than bulk Mg. Such an effect was originally explained as a consequence of elastic clamping on Mg by the capping Pd layer. An alternative interpretation later suggested that the pressure increase could originate from simple alloying between Mg and Pd. Here we resolve this controversy by measuring the hydrogenation and dehydrogenation isotherms of Mg-Pd thin film alloys over a wide range of compositions. Our results disentangle the effects of elastic clamping and alloying, and highlight the role of plastic deformations.

Several energy storage systems rely on the intercalation of solute atoms into solid host matrices. Tuning the thermodynamics of these solid state reactions is therefore of paramount importance for designing better energy storage materials [1–3]. For example, while magnesium hydride contains 7.6 mass% of hydrogen, its use in storage applications is limited by slow kinetics of hydrogen absorption and desorption and a high thermodynamic stability [4]. For this reason, several groups have studied ways to modify the stability of MgH_2 either via nanostructuring or by alloying with different elements [5–8]. In 2009, we have shown that Mg films covered with a thin layer of Mg-alloy-forming elements, such as Pd and Ni, absorb hydrogen at much higher H_2 gas pressures than bulk Mg [9]. We attributed such destabilization of MgH_2 to the elastic constraints imposed by the capping layer and developed a model to quantitatively interpret our data. In contrast to this explanation, Chung *et al.* have later proposed that the observed effect is a mere consequence of alloying at the Mg/Pd interface [10]. Here we solve this controversy by measuring the loading and unloading isotherms of Mg-Pd thin film alloys in a wide range of compositions. In particular, by comparing multiple loading cycles, we demonstrate that alloying with Pd does increase the hydrogenation pressure of Mg, but the effect is unrelated to the clamping mechanism observed for Pd- and Ni-capped films. Strikingly, neither the elastic clamping nor the alloying effects can account for the constant desorption pressure measured for all Mg-Pd alloy compositions. Such behavior points to the importance of plastic deformation and the creation of voids in the microstructure of the films upon cycling with hydrogen.

All thin films are deposited in an ultra-high vacuum DC/RF magnetron sputtering system (base pressure 10^{-7} Pa) in an argon atmosphere (6N purity, pressure 3 Pa), on substrates kept at room temperature. An $Mg_{1-x}Pd_x$ ($0.02 < x < 0.12$) gradient alloy layer is deposited between two Ti films and the samples are capped with a catalytic Pd layer (Fig. 1a). The Mg, Pd, and Ti targets have purity of 99.95%, 99.98%, and 99.999%, respectively. The Ti layers are intended to isolate the Mg-Pd alloy from the substrate and the palladium on top and minimize any elastic clamping effects [11]. As we will show, while Ti layers are very effective in elastically isolating pure Mg films [11], the negative enthalpy of mixing between Ti and Pd makes them less effective towards Mg-Pd alloys. The Mg-Pd alloy layer is deposited by angled co-sputtering of pure Mg and Pd targets on a 70x5x1 mm quartz wafer substrate. The thickness of the resulting alloy layer varies with composition due to the difference in total deposition rate of Mg and Pd along the 70 mm long substrate. The thickness of the $Mg_{1-x}Pd_x$ gradient alloy layer is measured with profilometry, while its composition is derived from the calibrated sputtering rates of pure Mg and Pd targets. Such calibration procedure has been validated using Rutherford backscattering spectrometry and it is known to provide reliable composition values

* a.baldi@differ.nl

[12]. The $Mg_{0.9}Pd_{0.1}$ samples for transmission electron microscopy (TEM) analysis are deposited on silicon nitride windows (20 nm thickness, 3x3 mm window array, TEMwindows.com). The Mg-Pd TEM samples have a uniform thickness of 50 nm while the Ti and Pd capping layers are all 3 nm thick, to minimize their influence during imaging. Planar view TEM images are recorded using a JEOL 2010F. Hydrogen absorption and desorption isotherms are measured using hydrogenography, a combinatorial technique that allows recording Pressure-optical Transmission Isotherms (PTIs) for a large number of alloy compositions at once [13]. In a PTI the amount of light transmitted by a thin film is measured as a function of increasing pressure at constant temperature. The hydrogenography setup consists of a stainless steel hydrogenation cell, which allows controlling the H_2 gas pressure between 10^1 and 10^6 Pa under a flow of 20 sccm. The cell has quartz windows for optical transmission measurements and is placed in a furnace to maintain a constant temperature (here between 333 K and 363 K). Depending on the experiment, we use pure hydrogen gas or mixtures containing 0.1% and 4% hydrogen in argon. The light transmitted by the thin films is continuously recorded with a 3-CCD camera (Sony) while varying the H_2 pressure at constant temperature (Fig. 1b). According to Beer-Lambert's law, the logarithm of the transmitted light, normalized by the transmission in the metallic state, is directly proportional to the hydrogen concentration in the film [14].

Figure 1c shows the loading PTIs for selected $Mg_{1-x}Pd_x$ compositions, recorded at 333 K during the first five hydrogenation cycles. Higher Pd concentrations lead to significantly higher loading pressures and smaller plateau widths. Interestingly, while for all compositions the loading pressure diminishes upon cycling, the width of the pressure plateaus, expressed in units of $\ln(T/T_0)$, remains roughly constant over multiple hydrogenation cycles (Fig. 2a). From Fig. 2a we also observe that the width of the pressure plateau depends on the Pd concentration in the Mg-Pd alloy. The decrease in plateau width with increasing Pd content is however only partially due to the variation in thickness across the Mg-Pd alloy sample. The solid line in Fig. 2a shows the plateau width expected under the assumption that Pd does not affect the hydrogen storage capacity of the Mg-Pd alloy and all Mg atoms hydrogenate to form MgH_2. This plateau width is calculated knowing that the hydrogenation of pure Mg to MgH_2 leads to an increase in $\ln(T/T_0)$ of $\sim$0.088 per nm of film thickness [11] (see also the Supplemental Material section SM1). From the discrepancy between the solid line and the measured plateau widths for all cycles, it is evident that the presence of Pd in the Mg-Pd alloy must prevent the absorption of a significant amount of hydrogen. Assuming that all Mg-Pd alloys form a MgH_2-like rutile structure upon hydrogenation [15, 16], in a fully hydrogenated sample each metal atom (Mg or Pd) will be surrounded by 6 hydrogen atoms. The dashed line in Fig. 2a plots the predicted plateau width if each Pd atom in the Mg-Pd alloy prevents the absorption of its 6 nearest neighbour hydrogen atoms. This corrected plateau width is calculated multiplying the "ideal" width (solid line) times a factor $(1-3x)$. The multiplication factor is correct in the limit of $x \ll 1$, i.e. in the limit of non-neighbouring Pd atoms (see also SM2). Assuming that each Pd atom prevents the absorption of $\sim$6 hydrogen atoms leads to predicted plateau widths close to the experimentally measured ones and indicates that *palladium significantly reduces the hydrogen storage capacity of Mg-Pd alloys*. As a consequence, the fact that the plateau widths for Mg-Pd thin films remain roughly constant for the first 5 hydrogen loadings indicates that *the overall composition and the chemical short-range order of the Mg-Pd alloys do not significantly change upon cycling* [12].

It is then interesting to look at the evolution of the equilibrium loading pressures over the first five hydrogenation cycles, as shown in Fig. 2b. We observe two distinct effects: *i*) in each cycle, higher Pd concentrations lead to higher loading pressures, and *ii*) upon cycling the loading pressure for all compositions decreases by more than an order of magnitude. In the following we demonstrate that the first effect can be quantitatively accounted for by the alloying of Mg and Pd.

Thin films of Mg-Pd alloys have a 002-oriented crystalline structure with x-ray diffraction peaks becoming broader and less intense with higher Pd concentrations and an average lattice parameter roughly corresponding to a Vegard mixture [15] (see SM3). In first approximation, we neglect electronic contributions to the enthalpy of hydride formation of $Mg_{1-x}Pd_x$ alloys and assume that the effect of mixing with Pd (molar volume $V_{Pd} = 8.8514$ cm^3/mol) is a mere contraction of the lattice of Mg (molar volume $V_{Mg} = 13.984$ cm^3/mol). Following Vegard's law, we can write the average contraction of the alloy's volume as

$$\frac{\partial \ln V}{\partial x} = \frac{V_{Pd} - V_{Mg}}{V_{Mg}} = -0.367 \tag{1}$$

The change in enthalpy of hydride formation as a function of composition is then given by [17]

$$\frac{\partial \Delta H}{\partial x} = \frac{\partial \Delta H}{\partial \ln V}\frac{\partial \ln V}{\partial x} = \\ = -B(x)V_H(x)\frac{\partial \ln V}{\partial x} = 0.367 B(x) V_H(x) \tag{2}$$

where $B(x)$ and $V_H(x)$ are the composition-dependent bulk modulus and hydrogen partial molar volume for the Mg-Pd alloy, respectively. The bulk modulus of the alloy is expressed as a simple weighted average of the bulk moduli of the constituent elements ($B_{Mg} = 35.4 \cdot 10^9$ Pa [18], $B_{Pd} = 181 \cdot 10^9$ Pa [18])

$$B(x) = (1-x)B_{Mg} + xB_{Pd} \tag{3}$$

while the partial molar volume of hydrogen in the alloy is taken as the partial molar volume of hydrogen in MgH_2 ($V_{H\ in\ MgH_2} = 2.24 \cdot 10^{-6}$ m^3/molH [9]), times the correction factor $(1-3x)$ that accounts for the reduced hydrogen storage capacity due to the presence of Pd

$$V_H(x) = V_{H\ in\ MgH_2}(1-3x) \tag{4}$$

It is easy to calculate that, for the range of compositions explored in the present paper, the product $B(x)V_H(x)$ is roughly constant and equal to 80 kJ/molH (see also SM4). From equation (2) we therefore have $\partial \Delta H/\partial x \approx 29$ kJ/molH. Using the van't Hoff relationship between the enthalpy of hydride formation, ΔH, and the hydrogen loading pressure, P_{H_2}, we finally obtain

$$\frac{\partial \ln P_{H_2}}{\partial x} = \frac{2}{RT}\frac{\partial \Delta H}{\partial x} \approx \frac{2 \cdot 29000 \text{ J/mol}}{8.314 \text{ J/(K} \cdot \text{mol)} \cdot 333 \text{ K}} \approx 21 \tag{5}$$

A linear fit to the composition dependence of the loading pressures for the fifth loading cycle in Fig. 2b yields a slope of ∼23, in excellent agreement with the predicted theoretical value. Note that a similar slope can also be extrapolated for the first loading cycle. *The effect of alloying between Mg and Pd can therefore be quantitatively accounted for by the observed dependence of the loading pressures on the Pd composition, x.*

By studying the loading isotherms of Mg-Pd alloy thin films we have so far demonstrated that *i*) alloying with Pd leads to higher loading pressures and to a significant reduction of hydrogen uptake in Mg thin films, and *ii*) cycling with hydrogen does not change the Mg-Pd composition. If the Pd content in Mg does not change upon cycling, however, *the decrease in the loading pressures of all Mg-Pd compositions upon multiple hydrogen loadings shown in Fig. 2b cannot be due to alloying effects and can only be attributed to (the removal of) elastic clamping effects*, as we originally proposed [9, 11].

During the first loading, the hydrogen-induced volume expansion of Mg-Pd thin films (32% for pure MgH_2 [19]) is constrained by the adjacent Ti layers, leading to very high hydrogenation pressures. Such elastic clamping is partially removed during subsequent cycles, due to hydrogen-induced plastic deformations and the creation of structural defects in the Mg-Pd film. This scenario is consistent with the measured broadening and decrease in intensity of the x-ray diffraction peaks of Mg-Pd thin film alloys observed upon hydrogen absorption [15]. Interestingly, Pd-poor compositions almost entirely relax these elastic constraints over one hydrogenation cycle, while Pd-rich composition have slower relaxation rates (Fig. 2b). This trend is consistent with the fact that Pd and Ti atoms form very stable alloys, with an enthalpy of mixing that is significantly more negative than that of Pd with Mg [20]. A larger Pd concentration in the Mg-Pd layer will therefore induce a stronger clamping by the adjacent Ti layers [9]. Furthermore, a higher Pd concentration significantly reduces the hydrogen uptake and the consequent plastic deformation of the film, leading to a slower relaxation rate upon cycling.

The lowering of elastic clamping effects upon hydrogen absorption should have dramatic consequences on the dehydrogenation mechanism. This is clearly shown in Fig. 3a, where we plot equilibrium PTIs for the first 3 loading cycles and for the 4$^{\text{th}}$ unloading cycle of a Mg-Pd alloy thin film. Since hydrogen desorption from thin films is typically slower than hydrogen absorption, the measurements were conducted at a higher temperature of 363 K, to accelerate the reaction kinetics and obtain equilibrium values also for the unloading isotherms [21]. Strikingly, while the loading pressures show a similar dependence on the film's composition as the ones measured at 333 K (Fig. 1), *the unloading equilibrium pressures do not exhibit any dependence on the Pd content.* The unloading mechanism must therefore be insensitive to the influence of alloying with Pd. In fact, the measured unloading pressure of 3 Pa at 363 K is very close to the one expected for bulk MgH_2 [22].

With the measurement of both loading and unloading isotherms, we can now attempt to draw a complete picture of the mechanism of hydrogen absorption and desorption in our Mg-Pd alloys. Upon hydrogen absorption, Mg-rich sites hydrogenate, while Pd-rich sites do not (Fig. 2a). This process decouples the hydrogenated MgH_2-like sites from the Pd-rich ones, which remain in their metallic state. Upon dehydrogenation the lattice volume decreases by ∼30% and the MgH_2-like sites are therefore free to desorb hydrogen without any constraint, leading to unloading equilibrium pressures that are independent on the film composition and close to the unloading pressure of pure MgH_2 (Fig. 3a) [16, 23]. Furthermore, the large volume expansion associated with the uptake of hydrogen must lead to macroscopic structural rearrangements. The associated increase in porosity will weaken the elastic clamping effect on the Mg-Pd alloy from the adjacent Ti layers. In contrast, the alloying influence of Pd is recovered after desorption, as evidenced by the constant slope of the curves in Fig. 2b. The formation of local structural defects upon hydrogen desorption has already been observed in pure Mg thin films, in which the volume contraction upon dehydrogenation is accompanied by the formation of a porous structure [24–26]. To corroborate this scenario we have collected planar view TEM images of a $Mg_{0.9}Pd_{0.1}$ alloy thin film before and after 10 hydrogenation cycles (Fig. 3b). These TEM images reveal drastic microstructural changes in the metal films upon hydrogen cycling, with coarsening of the grains and the formation of a large number of voids, as confirmed by the appearance of Fresnel fringes while imaging at over and under focus (not shown here). It is evident that the large expansion of Mg-based films upon hydrogenation is not fully relaxed on dehydrogenation and the formation of free surfaces (voids) is more favourable than the plastic deformation needed to fully

revert the film back to the initial compact state.

In the present work, we have shown that the effect of alloying between Mg and Pd on the hydrogenation pressure of Mg-Pd thin films can be fully accounted for by considering the volume contraction due to the addition of smaller Pd atoms to the Mg lattice. By applying the same reasoning to the case of Pd-capped thin films of pure magnesium [9], in which Mg and Pd form an alloy only at a very thin (less than 2 nm thick) Mg/Pd interface, it is clear that the alloying model of Chung *et al.* [10] cannot explain the observed large increases of hydrogen loading pressure for films as thick as 40 nm. Furthermore, as Mg and Ni have an enthalpy of mixing ($H^{mix}_{MgNi} = -5.6$ kJ/mol) that is an order of magnitude smaller than the one of Mg with Pd ($H^{mix}_{MgPd} = -43$ kJ/mol) [27, 28], the Chung *et al.*'s model would predict large differences for the loading pressures of Ni- and Pd-capped Mg films. This prediction is contrary to what observed experimentally [9]. Interstingly, our elastic clamping model predicts similar increases to the loading pressures of Ni- and Pd-capped Mg thin films, in agreement with the experimental observations. For a more detailed comparison between the clamping [9] and alloying [10] models see also the Supplemental Materials section SM5.

While the clamping model gives a reasonable estimate of the increase in loading pressures of capped thin films, it treats each layer within the elastic approximation and does not take into account any plastic deformation. In light of the composition-independent unloading isotherms shown in Fig. 3a, however, it is clear that treating the hydrogenation and dehydrogenation of Mg-based films within the elastic approximation is incorrect and that a rigorous treatment should include the energy involved in the creation of plastic deformations. Interestingly, such energy for pure Mg is comparable in magnitude to the elastic energy for a perfectly clamped Pd-Mg bilayer (see SM6), at least qualitatively explaining the success of the clamping model in reproducing the observed loading pressures. Finally, a similar asymmetric behavior between hydrogen loading and unloading has already been observed for palladium nanoparticles and interpreted as due to the formation of defects during hydrogen desorption [29].

In conclusion, we have presented a comprehensive study of the effect of alloying on the hydrogen absorption and desorption properties of Pd-doped Mg thin films. Our controlled sample geometry and combinatorial measurement scheme allow us to quantitatively disentangle the effect of alloying from the one due to clamping. Our results demonstrate that, while alloying Mg with Pd does contribute to an increase in loading pressure in Mg-Pd thin films, it cannot explain the 2 orders of magnitude increase in loading pressure observed for Pd-capped Mg films [9]. Our elastic clamping model, however, while quantitatively describing the observed increase in loading pressures, fails to explain why unloading isotherms do not show any composition dependence. Accurate modeling of the hydrogenation process of magnesium-based nanomaterials will have to include the large structural rearrangements and plastic deformations occurring upon hydrogen uptake. Furthermore, future efforts to use elastic clamping effects to destabilize hydrogen storage materials will have to take these observations into account. For example, rigid scaffolding systems can only effectively destabilize hydrogen storage systems that undergo small volume expansions upon hydrogenation, therefore remaining within the elastic regime. Alternatively, one could envision a scaffolding system composed of a hydrogen-transparent elastic polymer, capable of accommodating the large volume expansion associated with the hydrogenation process in Mg-based alloys. Finally, our work shows how essential it is that any claim about destabilization of storage materials is substantiated by absorption *and* desorption experiments [30].

ACKNOWLEDGMENTS

This work was supported by the Netherlands Organisation for Scientific Research (Nederlandse Organisatie voor Wetenschappelijk Onderzoek, NWO).

[1] W. Dreyer, J. Jamnik, C. Guhlke, R. Huth, J. Moškon, and M. Gaberšček, Nat. Mater. **9**, 448 (2010).
[2] M. R. Lukatskaya, B. Dunn, and Y. Gogotsi, Nat. Commun. **7**, 1 (2016).
[3] T. C. Narayan, A. Baldi, A. L. Koh, R. Sinclair, and J. A. Dionne, Nat. Mater. **15**, 768 (2016).
[4] L. Schlapbach and A. Zuttel, Nature **414**, 353 (2001).
[5] J. J. Vajo, F. Mertens, C. C. Ahn, R. C. Bowman, and B. Fultz, J. Phys. Chem. B **108**, 13977 (2004).
[6] R. W. P. Wagemans, J. H. Van Lenthe, P. E. De Jongh, A. J. Van Dillen, and K. P. De Jong, J. Am. Chem. Soc. **127**, 16675 (2005).
[7] H. Shao, M. Felderhoff, and F. Schuth, Int. J. Hydrogen Energy **36**, 10828 (2011).
[8] S. A. Shevlin and Z. X. Guo, J. Phys. Chem. C **117**, 10883 (2013).
[9] A. Baldi, M. Gonzalez-Silveira, V. Palmisano, B. Dam, and R. Griessen, Phys. Rev. Lett. **102**, 226102 (2009).
[10] C.-J. Chung, S.-C. Lee, J. R. Groves, E. N. Brower, R. Sinclair, and B. M. Clemens, Phys. Rev. Lett. **108**, 106102 (2012).
[11] A. Baldi, V. Palmisano, M. Gonzalez-Silveira, Y. Pivak, M. Slaman, H. Schreuders, B. Dam, and R. Griessen, Appl. Phys. Lett. **95**, 071903 (2009).
[12] R. Gremaud, A. Baldi, M. Gonzalez-Silveira, B. Dam, and R. Griessen, Phys. Rev. B **77**, 144204 (2008).
[13] R. Gremaud, C. P. Broedersz, D. M. Borsa, A. Borgschulte, P. Mauron, H. Schreuders, J. H.

Rector, B. Dam, and R. Griessen, Adv. Mater. **19**, 2813 (2007).
[14] R. Gremaud, M. Slaman, H. Schreuders, B. Dam, and R. Griessen, Appl. Phys. Lett. **91**, 231916 (2007).
[15] M. Pasturel, M. Slaman, H. Schreuders, J. Rector, D. Borsa, B. Dam, and R. Griessen, J. Appl. Phys. **100**, 023515 (2006).
[16] E. Callini, L. Pasquini, L. Rude, T. Nielsen, T. Jensen, and E. Bonetti, J. Appl. Phys. **108**, 073513 (2010).
[17] R. Griessen and R. Feenstra, J. Phys. F - Metal Phys. **15**, 1013 (1985).
[18] K. A. Gschneidner, Jr., Solid State Phys. **16**, 275 (1964).
[19] F. Manchester, *Phase Diagram of Binary Hydrogen Alloys* (ASM International, Materials Park, OH 44073-0002, 2000).
[20] A. R. Miedema, R. Boom, and F. R. de Boer, J. Less-Common Met. **41**, 283 (1975).
[21] L. P. A. Mooij, A. Baldi, C. Boelsma, K. Shen, M. Wagemaker, Y. Pivak, H. Schreuders, R. Griessen, and B. Dam, Adv. Energy Mater. **1**, 754 (2011).
[22] Y. Pivak, H. Schreuders, and B. Dam, Crystals **2**, 710 (2012).
[23] J. Dufour and J. Huot, J. Alloys Compd. **446-447**, 147 (2007).
[24] J. A. Dura, S. T. Kelly, P. A. Kienzle, J. H. Her, T. J. Udovic, C. F. Majkrzak, C.-J. Chung, and B. M. Clemens, J. Appl. Phys. **109**, 093501 (2011).
[25] L. Mooij and B. Dam, Phys. Chem. Chem. Phys. **15**, 2782 (2013).
[26] L. J. Bannenberg, H. Schreuders, L. van Eijck, J. R. Heringa, N.-J. Steinke, R. Dalgliesh, B. Dam, F. M. Mulder, and A. A. van Well, J. Phys. Chem. C **120**, 10185 (2016).
[27] F. R. de Boer, R. Boom, W. C. M. Mattens, A. R. Miedema, and A. K. Niessen, *Cohesion in Metals: Transition Metal Alloys* (North-Holland, Amsterdam, 1989).
[28] A. Debski, R. Debski, and W. Gasior, Archives of Metallurgy and Materials **59**, 1337 (2014).
[29] R. Griessen, N. Strohfeldt, and H. Giessen, Nat. Mater. **15**, 311 (2016).
[30] P. Ngene, A. Longo, L. Mooij, W. Bras, and B. Dam, Nat. Commun. **8**, 1846 (2017).

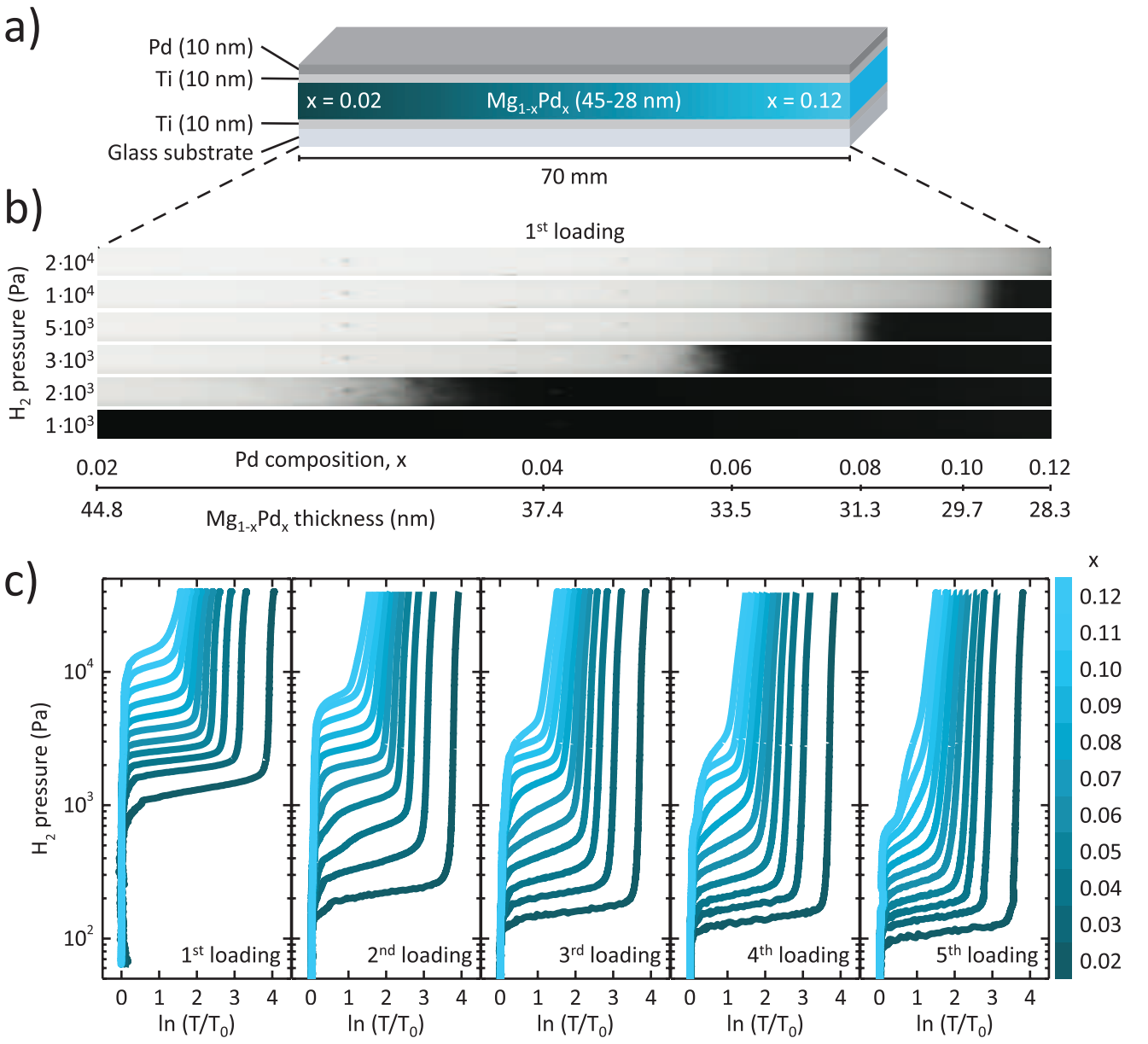

FIG. 1. (Color online) a) Sketch of the sample used to measure the hydrogen loading and unloading isotherms of $Mg_{1-x}Pd_x$ alloys ($0.02 < x < 0.12$) in the hydrogenography setup. b) Top-view optical transmission images collected through the sample at increasing H_2 pressures at 333 K. The images have been stretched horizontally for clarity. c) Loading PTIs measured at 333 K for selected Mg-Pd alloy compositions in the first five hydrogenation cycles.

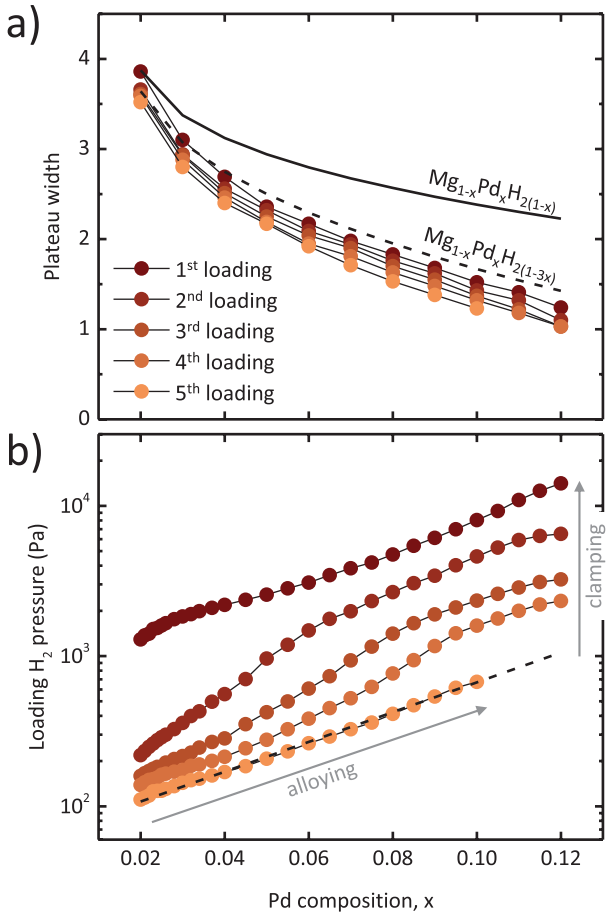

FIG. 2. (Color online) a) Width of the nearly horizontal loading plateaus expressed in units of $\ln(T/T_0)$ for the isotherms shown in Fig. 1c. The solid line corresponds to the expected plateau width, if all the Mg atoms in the Mg-Pd alloy would hydrogenate to form the dihydride MgH_2. The dashed line corresponds to the expected plateau width for a random Mg-Pd alloy in which each Pd atom prevents H occupation of the 6 nearest neighboring sites. b) Average loading pressures as a function of Pd atomic composition for the first 5 loading cycles. The dashed line is a linear fit to the "$\ln P$ vs x" plot during the 5^{th} loading. The fit gives a slope of $\sim$23.

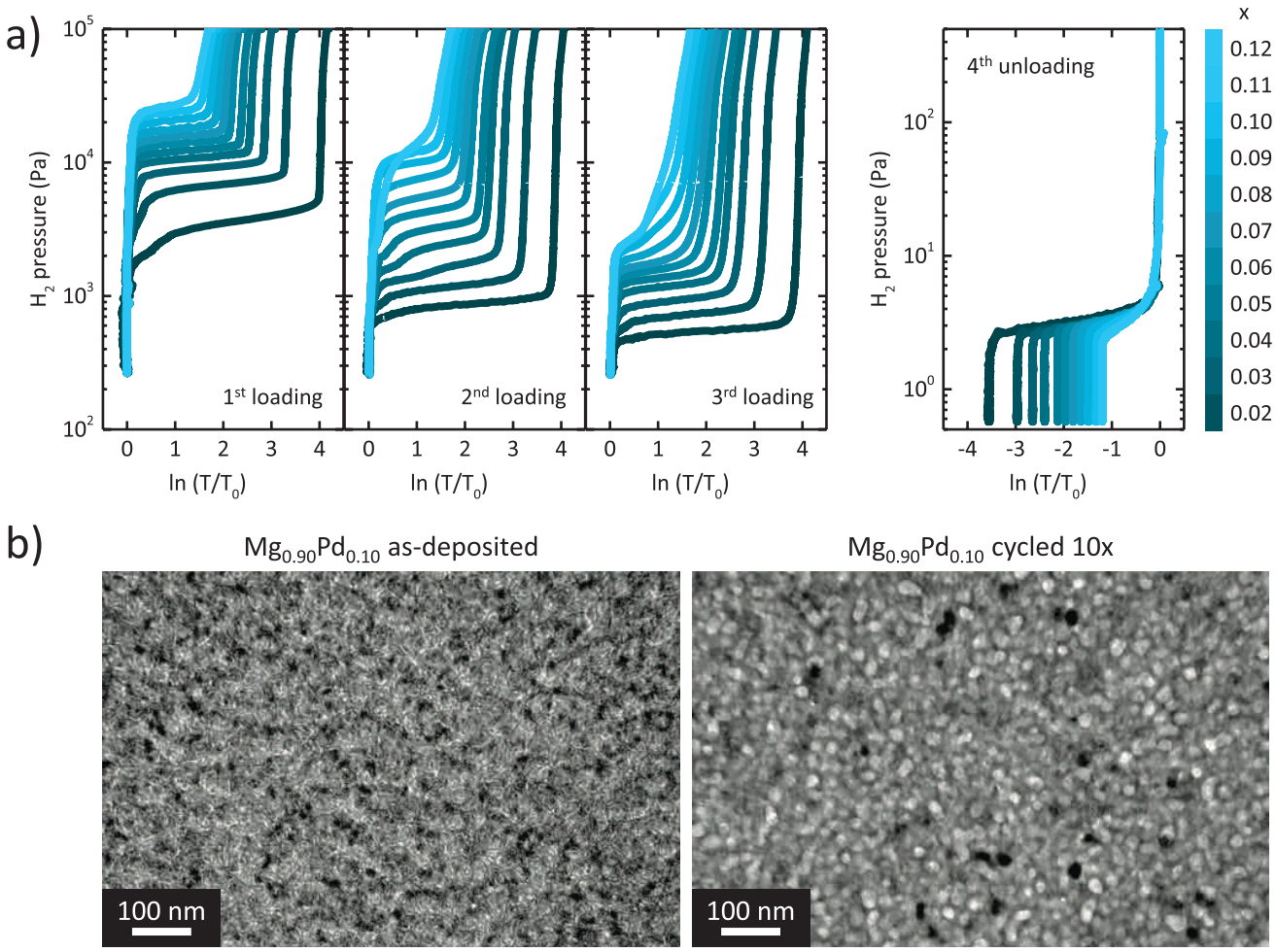

FIG. 3. (Color online) a) Pressure-transmission-isotherms (PTIs) measured at 363 K for the Mg-Pd thin films for the first three loading and the fourth unloading. Note the different H_2 pressure range for the unloading cycle. b) Planar view TEM images of a $Mg_{0.9}Pd_{0.1}$ film (left) before and (right) after 10 hydrogenation and dehydrogenation cycles. The sample is supported by a thin Si_3N_4 membrane and the contribution of the Ti and Pd layers has been minimized using the following structure: Si_3N_4/Ti (2nm)/$Mg_{0.9}Pd_{0.1}$ (50nm)/Ti (2nm)/Pd (3nm).